6-22-2012

Potential Role of Inorganic Polyphosphate in the Cycling of Phosphorus Within the Hypoxic Water Column of Effingham Inlet, British Columbia

Julia M. Diaz

Ellery D. Ingall

Samuel D. Snow

Claudia R. Benitez-Nelson
benitezn@mailbox.sc.edu

Martial Taillefert

See next page for additional authors

Publication Info

Published in *Global Biogeochemical Cycles*, Volume 26, Issue 2, 2012.

Potential role of inorganic polyphosphate in the cycling of phosphorus within the hypoxic water column of Effingham Inlet, British Columbia

Julia M. Diaz,[1,2] Ellery D. Ingall,[1] Samuel D. Snow,[1,3] Claudia R. Benitez-Nelson,[4] Martial Taillefert,[1] and Jay A. Brandes[5]

Received 29 September 2011; revised 13 April 2012; accepted 7 May 2012; published 22 June 2012.

[1] The upper basin of Effingham Inlet possesses permanently anoxic bottom waters, with a water column redox transition zone typically occurring at least 40 m above the sediment-water interface. During our sampling campaign in April and July 2007, this redox transition zone was associated with sharp peaks in a variety of parameters, including soluble reactive phosphorus (SRP) and total particulate phosphorus (TPP). Based on sequential extraction results, TPP maxima exhibited preferential accumulation of an operationally defined class of loosely adsorbed organic phosphorus (P), which may contain a substantial fraction of polyphosphate (poly-P). This poly-P may furthermore be involved in the redox-dependent remobilization of SRP. For example, direct fluorometric analysis of poly-P content revealed that particulate inorganic poly-P was present at concentrations ranging from 1 to 9 nM P within and several meters above the TPP maximum. Below the depth of 1% oxygen saturation, however, particulate inorganic poly-P was undetectable (<0.8 nM in situ). Assuming this concentration profile reflects the remineralization of inorganic poly-P to SRP across the redox transition, inorganic poly-P degradation accounted for as much as 4 ± 3% (average ± standard deviation) to 9 ± 8% of the vertical turbulent diffusive SRP flux. This finding is a conservative estimate due in part to sample storage effects associated with our analysis of poly-P content. By comparison, iron-linked P cycling accounted for at most 65 ± 33% of the diffusive SRP flux, leaving ∼25% unaccounted for. Thus, while redox-sensitive poly-P remineralization in Effingham Inlet appears modest based on our direct conservative estimate, it may be higher from a mass balance viewpoint. Poly-P cycling may therefore be an overlooked mechanism for the redox-sensitive cycling of P in some hypoxic/anoxic boundaries, especially iron-poor marine oxygen minimum zones.

Citation: Diaz, J. M., E. D. Ingall, S. D. Snow, C. R. Benitez-Nelson, M. Taillefert, and J. A. Brandes (2012), Potential role of inorganic polyphosphate in the cycling of phosphorus within the hypoxic water column of Effingham Inlet, British Columbia, *Global Biogeochem. Cycles*, *26*, GB2040, doi:10.1029/2011GB004226.

1. Introduction

[2] Phosphorus (P) is a vital nutrient present in essential biomolecules such as DNA, phospholipids, and ATP. In the marine environment, P is considered the ultimate limiting nutrient over geologic timescales because slow tectonic processes control its input to the ocean, and the inputs of other nutrients are rapid by comparison (e.g., biological fixation of atmospheric N_2) [*Algeo and Ingall*, 2007; *Broecker*, 1982; *Redfield*, 1958; *Van Cappellen and Ingall*, 1996]. Mounting evidence over the last several decades has shown that P is also present at limiting concentrations in vast regions of the modern ocean, leading to a growing need for a better understanding of the short-term P cycle [*Benitez-Nelson*, 2000; *Paytan and McLaughlin*, 2007].

[3] A widespread process in P biogeochemistry is the enhanced remobilization of P from oxic-anoxic transition zones, which has been observed in lacustrine and marine systems and in modern and ancient sediments [*Golterman*, 2001; *Hupfer et al.*, 1995; *Ingall and Jahnke*, 1994, 1997; *Ingall et al.*, 1993; *Slomp et al.*, 2002]. This process contributes to the redox stabilization of the atmosphere and

[1]School of Earth and Atmospheric Sciences, Georgia Institute of Technology, Atlanta, Georgia, USA.
[2]Now at School of Engineering and Applied Sciences, Harvard University, Cambridge, Massachusetts, USA.
[3]Now at School of Civil and Environmental Engineering, Georgia Institute of Technology, Atlanta, Georgia, USA.
[4]Marine Science Program and Department of Earth and Ocean Sciences, University of South Carolina, Columbia, South Carolina, USA.
[5]Skidaway Institute of Oceanography, Savannah, Georgia, USA.

Corresponding author: J. M. Diaz, School of Engineering and Applied Sciences, Harvard University, 58 Oxford St., ESL Rm. 228, Cambridge, MA 02138, USA. (jdiaz@seas.harvard.edu)

0886-6236/12/2011GB004226

oceans over geologic time [*Van Cappellen and Ingall*, 1996]. Over a period of years to centuries, however, enhanced hypoxic/anoxic P regeneration exacerbates ecological problems associated with anthropogenic eutrophication [*Jilbert et al.*, 2011; *Savchuk et al.*, 2008; *Vahtera et al.*, 2007], resulting in elevated water column P concentrations, changing nitrogen (N) fixation patterns, and devastating impacts on native macrofauna and fisheries industries [*Jilbert et al.*, 2011; *Vahtera et al.*, 2007]. Because eutrophication likely leads to P-limited systems [*Codispoti et al.*, 2001; *Rabalais et al.*, 2002], combined with the fact that marine oxygen minimum zones are expanding due to human activity [*Naqvi et al.*, 2000; *Rabalais et al.*, 2001; *Stramma et al.*, 2008], the biogeochemical impacts of enhanced hypoxic/anoxic P regeneration have a strong potential to alter global ecosystem function and the global nutrient cycles of P, N, and associated elements.

[4] Despite the significant impacts of enhanced anoxic P regeneration on the global environment over both geologic and modern timescales, the underlying mechanisms of this process are not fully understood. A rich set of previous observations suggest that P regeneration mechanisms are decoupled from those of carbon (C) and N under hypoxic/anoxic conditions [*Golterman*, 2001; *Hupfer et al.*, 1995; *Ingall and Jahnke*, 1994, 1997; *Ingall et al.*, 1993; *Jilbert et al.*, 2011; *Slomp et al.*, 2002]. For example, the classic explanation of enhanced anoxic P regeneration involves the reductive dissolution of iron (Fe) oxyhydroxide mineral particles. Under oxic conditions, Fe oxyhydroxides are efficient surfaces for P adsorption and therefore act as a sink for dissolved P. Under anoxic conditions, however, Fe oxyhydroxides are unstable, resulting in the release of dissolved P. Although this Fe mechanism is a common and well-studied process [e.g., *Froelich et al.*, 1979; *McManus et al.*, 1997; *Mortimer*, 1941, 1942; *Sundby et al.*, 1992], its global contribution to the enhanced hypoxic/anoxic regeneration of P remains poorly constrained. In fact, Fe-linked P cycling is insufficient to account for redox-sensitive P regeneration in some sedimentary environments [*Golterman*, 2001; *Ingall et al.*, 2005; *Jilbert et al.*, 2011] and water column redox transition zones [*Jilbert et al.*, 2011; *Turnewitsch and Pohl*, 2010].

[5] An additional potential mechanism for redox-sensitive P cycling in aquatic environments is polyphosphate (poly-P) cycling by bacteria. Poly-P is a linear polymer of at least three orthophosphate molecules linked by high-energy phosphoanhydride bonds [*Brown and Kornberg*, 2004; *Kornberg*, 1995]. In biological cells, poly-P can be organic, as in the case of trinucleotides such as ATP, or inorganic. Inorganic poly-P typically ranges in size from three to several hundreds of P atoms [*Kornberg*, 1995]. It is a common biomolecule found in every type of cell, and its biological purpose is multifunctional, including storage of P and energy [*Kornberg*, 1995; *Kornberg et al.*, 1999; *Rao et al.*, 2009].

[6] In ocean environments both bacteria [*Schulz and Schulz*, 2005] and phytoplankton [*Diaz et al.*, 2008] are sources of inorganic poly-P. However, as a group, only bacteria are known for the ability to remineralize inorganic poly-P in a redox-sensitive manner. For example, poly-P is a redox-sensitive molecule in the poly-P accumulating bacteria (PAB) that are utilized for enhanced biological P removal during wastewater treatment [*Comeau et al.*, 1986; *Nielsen et al.*, 2010; *Schuler and Jenkins*, 2003; *Seviour et al.*, 2003]. In these systems, PAB cultivated under anaerobic conditions remineralize endogenous reserves of inorganic poly-P, presumably using the P and energy released from depolymerization as a source for ATP in the absence of oxygen as a terminal electron acceptor. Upon exposure to oxygen, the PAB-dominated community removes P from the aqueous environment in order to reform intracellular inorganic poly-P reserves, producing a system deplete in dissolved P and rich in particulate P, which can be filtered and removed [*Comeau et al.*, 1986; *Nielsen et al.*, 2010; *Schuler and Jenkins*, 2003; *Seviour et al.*, 2003]. To our knowledge, the redox-sensitive remineralization of exogenous (e.g., phytoplankton derived) inorganic poly-P by bacteria has not been observed. In fact, the general bioavailability of exogenous inorganic poly-P remains unknown.

[7] A bacterially driven process analogous to enhanced biological phosphorus removal may be contributing to the redox-sensitive cycling of P in aquatic systems [*Hupfer et al.*, 1995, 2004; *Ingall and Jahnke*, 1997; *Sannigrahi and Ingall*, 2005]. Poly-P metabolism occurs along a redox potential range that overlaps microbially mediated iron reduction [*Davelaar*, 1993]. Thus, P distribution and fluxes in redox transitions attributed to the coupled cycling of iron and phosphate may include some component of poly-P metabolism. Although poly-P has been previously shown to represent a substantial portion of the total P in marine systems and our current study site in particular [*Diaz et al.*, 2008; *Sannigrahi and Ingall*, 2005; *Young and Ingall*, 2010], the potential redox-sensitive cycling of this chemical species has remained enigmatic and historically eluded direct detection [*Davelaar*, 1993; *Gächter et al.*, 1988; *Golterman*, 2001; *Hupfer et al.*, 1995, 2004, 2008; *Sannigrahi and Ingall*, 2005; *Schulz and Schulz*, 2005]. Here, we utilize field observations collected during two seasons in Effingham Inlet, British Columbia, to clarify the potential role played by poly-P in the redox-sensitive remineralization of P.

2. Methods

2.1. Study Site

[8] Field observations were collected during April and July 2007 from Effingham Inlet, a fjord located on the west coast of Vancouver Island, British Columbia (Figure 1). Effingham Inlet is a very narrow basin with dynamic bottom topography, including a shallow (40 m) sill present at the entrance to the upper basin, which restricts vertical circulation in this area, leading to persistent bottom water anoxia. The location of the water column redox transition zone in this 120 m deep basin varies across seasons but is typically present between 60 and 80 m depth.

2.2. Sample Collection and Analysis

[9] Seawater samples and in situ data were collected aboard the R/V *Barnes* using a CTD rosette sampler. Dissolved oxygen concentrations and physical properties of the seawater such as temperature and salinity were measured continuously during each cast, and these data were processed using the SEASOFT software (Seabird Electronics, Inc., Washington, USA). The water column redox transition zone was defined as the depth range corresponding to 1–10%

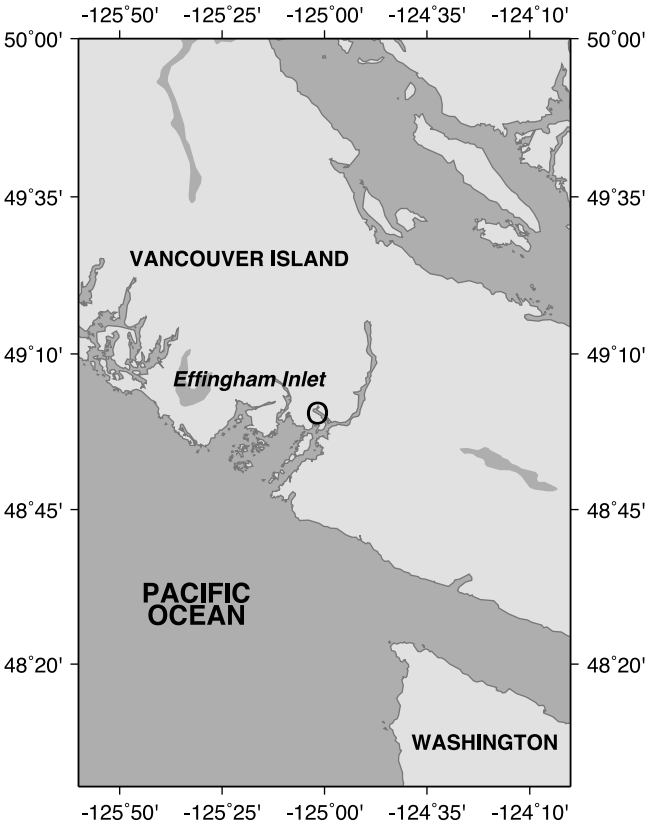

Figure 1. Effingham Inlet. Two sampling campaigns were conducted during April and July 2007 in the upper basin of Effingham Inlet, Vancouver Island, British Columbia, located at 49°4′N, 125°9′W.

oxygen saturation, where the concentration of dissolved oxygen in the surface 1–2 m was assumed to be the 100% oxygen saturation level.

[10] Water samples for soluble reactive P (SRP) were syringe filtered (0.45 μm) and analyzed in the field according to standard colorimetric protocols [*Hansen and Koroleff*, 1999]. Measurements of SRP typically exhibited errors of <3%. Water samples for bacterial counts were fixed in 2% formaldehyde and filtered onto polycarbonate membrane filters (0.2 μm). Cells were counted on an Olympus epifluorescence microscope after staining with 4′,6′-Diamidino-2-phenylindole (DAPI).

[11] Particles were collected from seawater onto GF/F filters (Whatman) and size fractionated between 1 μm and 10 μm using an in situ McLane pump. Particulate P was quantified using the procedure of *Aspila et al.* [1976]. Duplicate measurements of particulate P agreed to within <5%, and the measured value of NIST Standard Reference Material 1573a (tomato leaves) was within ±5% of the certified value.

[12] Total particulate C (PC) and N (PN) were determined with an elemental analyzer (Costech Analytical Technologies, Inc.). Samples for particulate organic C (POC) and nitrogen (PON) were prepared according to the vapor acidification approach of *Hedges and Stern* [1984]. The error associated with the measurement of C and N by this method is typically ±15% and ±6%, respectively.

[13] Extractable Fe analysis was performed following 24 h extraction of the filtered material into a basic solution of 5% bicarbonate, 5% citrate, and 2% ascorbic acid, subsequent acidification to pH 1, and analysis on a flame atomic adsorption spectrometer. The typical analytical error associated with this measurement is ±5–10%.

[14] P speciation of particles collected in the 1–10 μm size fraction was assessed using the P sequential extraction procedure (SEDEX) developed by *Ruttenberg* [1992]. As a modification of the original SEDEX protocol, we measured both the organic and inorganic P of every SEDEX fraction. Error associated with the measurement of organic P in SEDEX fractions was ±31%, whereas the error associated with the measurement of inorganic P in SEDEX fractions was ±24%.

[15] Direct quantification of particulate inorganic poly-P in the 1–10 μm size range was accomplished using a recently developed fluorometric protocol based on the interaction of inorganic poly-P with DAPI [*Aschar-Sobbi et al.*, 2008; *Diaz and Ingall*, 2010]. DAPI is commonly utilized as a stain for nucleic acid but will also bind poly-P, which can be detected at a characteristic wavelength. Using a combination of incident and observed wavelengths optimized for specificity and sensitivity for poly-P detection [*Aschar-Sobbi et al.*, 2008], inorganic poly-P of at least 15 P atoms in size is quantified independently of chain length to a detection limit of 0.5 μM [*Diaz and Ingall*, 2010]. Typical errors associated with this technique are ±15% [*Diaz and Ingall*, 2010].

[16] Particulate samples for inorganic poly-P analysis were stored approximately 3 years before development of the fluorometric technique. These samples may have therefore undergone an unknown degree of poly-P degradation in this time, based on the finding that aqueous sodium poly-P standards are subject to observable decomposition over 10–15 days [*Diaz and Ingall*, 2010]. Based on the unknown storage effect on our samples and the chain length specificity of the fluorometric method, our inorganic poly-P measurements represent minimum estimates.

3. Results and Discussion

3.1. Oxygen

[17] Sampling during April and July 2007 occurred during and after the spring bloom, respectively. Consistent with the rapid consumption of oxygen (O_2) coupled to the oxidation of abundant organic matter produced during bloom conditions, the position of the water column redox transition (1–10% O_2 saturation) was higher in April (60.3 ± 1.0 (average ± standard deviation) m to 64.8 ± 0.5 m) than during postbloom sampling in July (68.7 ± 2.1 m to 76.7 ± 1.5 m). In the April sampling season, the redox transition zone ranged from 31 ± 3 to 317 ± 99 μg O_2 L^{-1}. Similarly, the redox transition zone ranged from 34 ± 7 to 370 ± 27 μg O_2 L^{-1} in the July sampling season (Figure 2).

3.2. Dissolved and Particulate P, POC, PON, and Bacterial Abundance

[18] In both seasons, particulate P and SRP exhibited sharp peaks in concentration (<10 m breadth) within the redox transition (Figure 3). The maximum concentration of

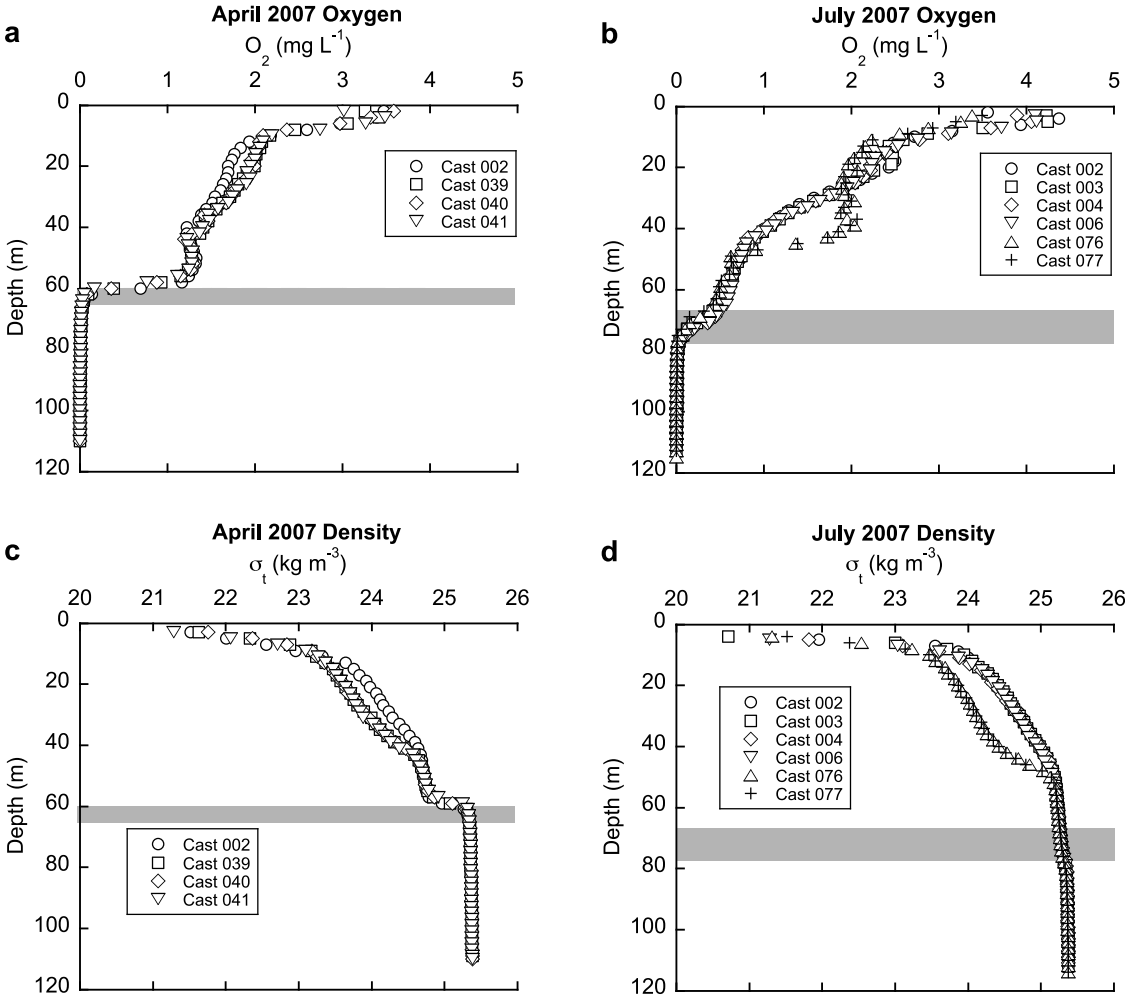

Figure 2. Density and dissolved oxygen profiles. The hypoxic transition is defined as the region between 1% and 10% oxygen saturation, or approximately 30–300 μg L^{-1}. This zone occurred between approximately (a) 60 and 65 m in April 2007 and (b) 69 and 77 m in July 2007 (shaded regions). In both seasons the redox transition coincided with a pycnocline, which was stronger in (c) April than in (d) July.

total particulate phosphorus (TPP) in the 1–10 μm size fraction was observed at 61 m and 77 m in the April and July sampling seasons, respectively (Figure 3). An overlapping peak in SRP occurred at 60 m in April and 75–76 m in July (Figure 3). The average peak concentration of TPP and SRP in both seasons was 1.13 $\pm$ 0.09 μM and 4.5 $\pm$ 0.4 μM, respectively. The gradients in TPP and SRP concentration on either side of these peaks were steep. For example, TPP exhibited an average concentration gradient of 0.25–0.5 μM m^{-1} across both seasons, whereas SRP displayed an average gradient of 0.13–0.63 μM m^{-1}.

[19] As expected, the hypoxic transition zone coincided with a pycnocline in both seasons (Figure 2). The density gradient in April (91.2 $\pm$ 10.5 g m^{-4}) was stronger than in July (6.7 $\pm$ 0.4 g m^{-4}). However, in either season, the dramatic patterns in P distribution cannot be explained by simple particle settling alone. For example, although particulate C and N also exhibited peaks in concentration within the redox transition zone (Figure 4), particulate elemental ratios in the 1–10 μm size fraction indicate that P accumulates independently of C and N. Outside the redox transition, average atomic ratios of particulate C:P, N:P, and C:N across both seasons were 137.9 $\pm$ 92.8, 22.7 $\pm$ 15.4, and 7.1 $\pm$ 3.5, respectively (Figure 5). A two-sided t test revealed that the C:P ratio was consistent with the revised Redfield composition of *Anderson and Sarmiento* [1994] (Redfield C:P = 117; p = 0.19; T = 1.33; n = 35), as was the C:N ratio (Redfield C:N = 6.625; p = 0.39; T = 0.88; n = 35). In contrast, the average C:P and N:P ratios within the hypoxic transition zone (44.2 $\pm$ 22.3 and 8.33 $\pm$ 4.0, respectively) were each $\sim$65% lower than the particulate C:P and N:P composition of vertically adjacent waters (Figure 5), a statistically significant decrease (p = 0.0002; T = 4.09; n = 52) and (p = 0.0004, T = 3.75; n = 52), respectively. However, C:N ratios within the redox transition (5.2 $\pm$ 0.7) were only $\sim$30% lower than the particulate C:N composition in adjacent waters, as reflected in the relatively conservative depth profile of C:N (Figure 5). These elemental ratios indicate that P is preferentially accumulated in particulate matter relative to C and N at the hypoxic transition zone.

[20] In addition to particulate elemental ratios, particulate P concentrations normalized to bacterial cell abundance

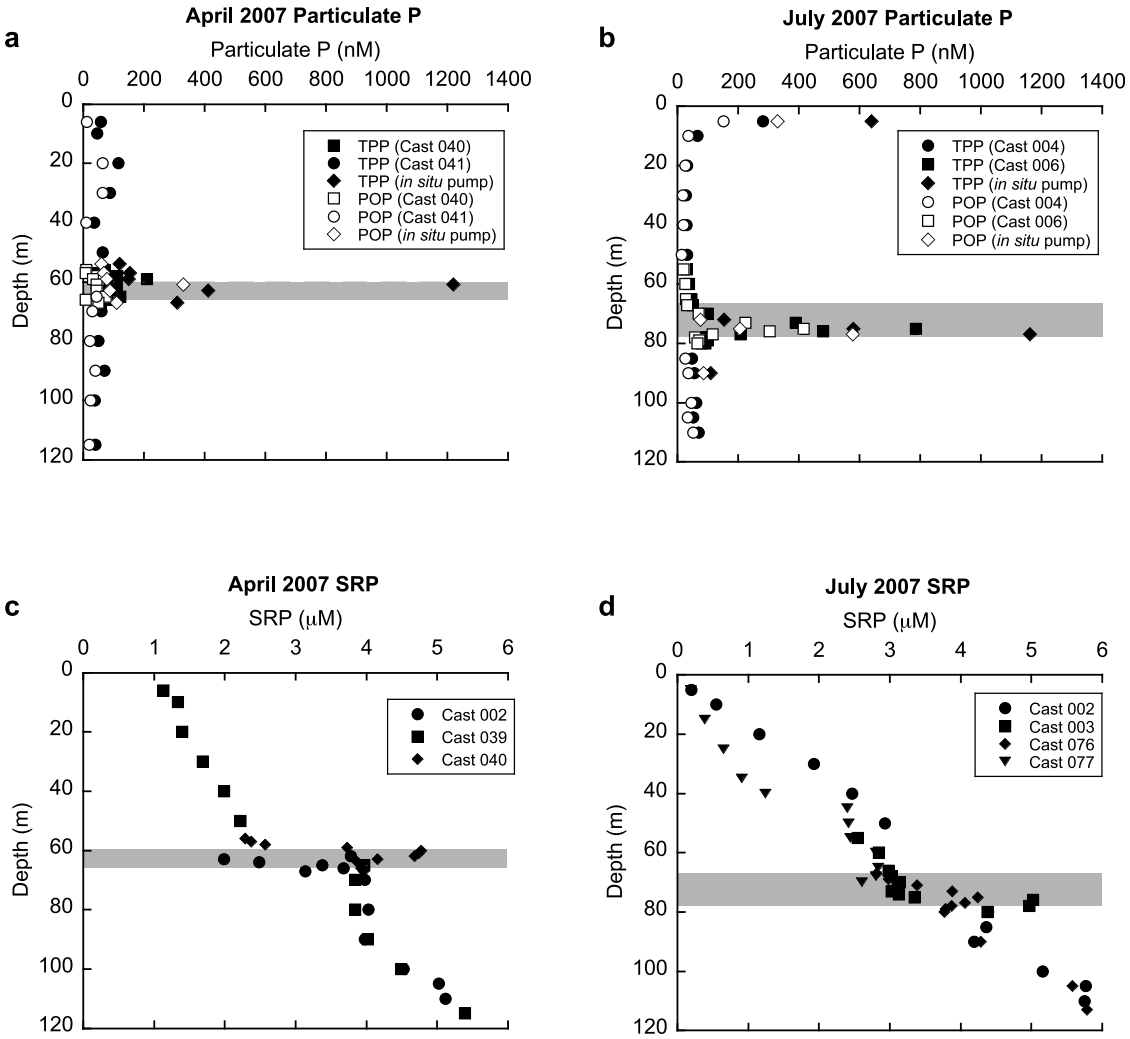

Figure 3. Phosphorus distributions. (a and b) Concentrations of total particulate P (TPP) and particulate organic P (POP) and (c and d) soluble reactive P (SRP) exhibited local maxima within the hypoxic transition zone (shaded regions) in both sampling seasons. Particulate P and SRP measurements exhibited errors of less than ±5% and ±3%, respectively.

also show a depth-dependent trend, with the concentration of TPP expressed per cell increasing threefold to fivefold within the redox transition (Figure 6). If the fraction of P unassociated with bacterial cells is assumed to be constant with depth, this finding suggests that the in situ bacterial community may store excess P under anoxic conditions relative to their constitutive demand under redox-stable conditions. Why this excess P storage may occur, especially in a redox-sensitive and therefore depth-dependent manner, is not well understood, nor is it intuitive given the high concentration of exogenous, bioavailable SRP. However, this pattern is nevertheless consistent with the conceptual models of enhanced biological phosphorus removal in wastewater treatment systems.

[21] Although discrepancies in particulate C content between Niskin bottle and in situ pump sampling methodologies have been reported previously [*Liu et al.*, 2005, 2009; *Moran et al.*, 1999], several factors may explain the relative consistency we observe between results from these two methods (Figures 3 and 4). For instance, size fractionation of our in situ pump samples (1–10 μm) may help to reconcile results from these two methods. Furthermore, particulate N and P estimates may be subject to inherently smaller discrepancies than those previously reported for C, especially in the size fraction examined. The high degree of productivity observed in our study site may also serve mitigate potential inconsistencies between the two sampling methods.

3.3. P Speciation

[22] On average across both seasons and all sampling depths, the majority of P in the 1–10 μm size fraction (97.6 ± 5.6%) was recovered in the loosely sorbed, Fe-bound, and recalcitrant organic P fractions, the first, second, and fifth steps of the SEDEX procedure, respectively. The loosely sorbed P fraction alone accounted for an average of 69.4 ± 18.4% of total extracted P across all samples. Detrital and authigenic P concentrations were at or below detection. Although every SEDEX P fraction exhibited local maxima at the depth corresponding to peak TPP (Figure 7),

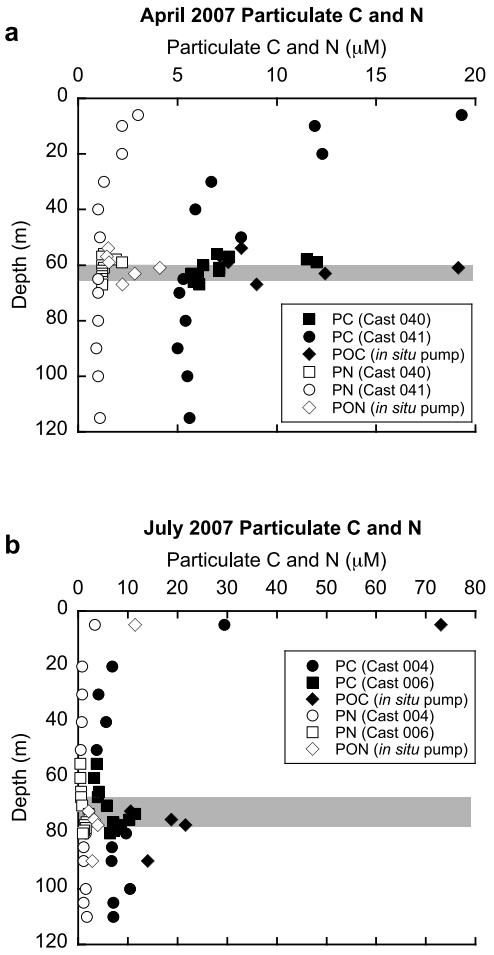

Figure 4. Carbon and nitrogen distributions. Concentrations of total particulate C (PC) and N (PN) and particulate organic C (POC) and N (PON) exhibited local maxima within the hypoxic transition zone (shaded regions) in (a) April and (b) July sampling seasons. Errors associated with the measurement of particulate C and N were typically ±15% and ±6%, respectively.

changes in TPP content were driven primarily by shifting concentrations of loosely sorbed P (Figure 7).

[23] Across both sampling seasons, the TPP maximum measured in the 1–10 μm size fraction was 80.4 ± 0.1% in excess, or 908.7 ± 0.1 nM P higher than the concentration of TPP expected at this depth based on Redfield stoichiometry and the concentrations of particulate C and N. As seen in the plots of relative concentration (Figure 7), SEDEX results did not reveal a single P fraction that could account for the entire excess or non-Redfieldian TPP observed in either sampling season. In fact, based on its profile of TPP-normalized content, adsorbed organic P was the only SEDEX P pool that appeared to be preferentially accumulated within the TPP maximum in both seasons (Figure 7). For example, loosely adsorbed organic P increased from an average of 10 to 32% of TPP in the TPP max during April 2007 and from 35 to 61% of TPP in July 2007, for an average relative increase of 23 ± 3%. Thus in each season, approximately 23% of the TPP maximum represents the fraction of organic adsorbed P that has been accumulated in excess of the composition of vertically adjacent waters. The remaining ~77% of the TPP maximum in either season is therefore due to the near-proportional increase in all of the other P species at that depth, e.g., adsorbed inorganic P, oxide associated P, and recalcitrant organic P. More of the TPP within the P maxima can possibly be attributed to P speciation shifts than our findings indicate, as the SEDEX method may not sufficiently delineate changes in P composition within broad extraction groups, e.g., between specific compounds within the fraction identified as "loosely sorbed P."

[24] The recalcitrant organic P and Fe-bound P fractions follow a pattern consistent with redox-sensitive degradation based on their profiles of relative concentration (Figure 7). Indeed, Fe oxyhydroxide-bound SRP decreased from 40 ± 8 nM P within and several meters above the TPP maximum to 6 ± 1 nM P below across both seasons. Despite this relatively low P concentration, the atomic ratio of total Fe-bound P to total particulate Fe (P:Fe) was ~0.2–0.6 above the redox transition, which is relatively high compared to the typical P:Fe ratio in modern, fully oxygenated sediments (~0.03) [*Planavsky et al.*, 2010].

[25] In contrast to the redox-sensitive drop in Fe-bound P content, decreases in the relative content of recalcitrant organic P across the hypoxic transition zone are driven by increases in TPP rather than absolute decreases in this P pool. For example, the content of recalcitrant organic P within and several meters above the TPP maximum was 43 ± 9 nM P and remained relatively unchanged at 36 ± 7 nM P below.

[26] The large (23%) preferential accumulation of organic adsorbed P within the TPP max is consistent with preferential biological synthesis of not only a variety of organic P species but also inorganic poly-P, which is typically detected in operationally defined "organic P" pools. Previous measurements of poly-P content within the Effingham Inlet water column have revealed that poly-P accounts for approximately 7–23% of TPP in plankton, sinking particles, and dissolved matter based on ^{31}P-NMR [*Diaz et al.*, 2008] and fluorometric analysis [*Diaz and Ingall*, 2010]. In contrast, our current results from the fluorometric analysis of suspended particles (1–10 μm fraction) indicate that inorganic poly-P is a substantially lower fraction of the total P in this pool (~1%). For instance, the inorganic poly-P content of 1–10 μm particles 2 m above the TPP max was 1 nM P, increasing to an average concentration of 9 nM P within the TPP max, and decreasing to below detection ~15 m below the hypoxic transition zone (<0.8 nM P in situ).

[27] The disappearance of inorganic poly-P from the 1–10 μm particulate fraction in anoxic waters is in contrast to previous results indicating the stability of inorganic poly-P in the anoxic zone. For example, previous results revealed comparable levels of dissolved poly-P in oxic and anoxic waters, and the vertical transport of diatom-encased poly-P through anoxic waters has been observed in Effingham Inlet [*Diaz et al.*, 2008]. Thus, the apparent redox-sensitive remobilization of inorganic poly-P seems to not only be a function of particle association, and therefore consistent with biological control, but also of particle size.

[28] The decreasing inorganic poly-P content of 1–10 μm particles is also consistent with the hypothesis that bacterial

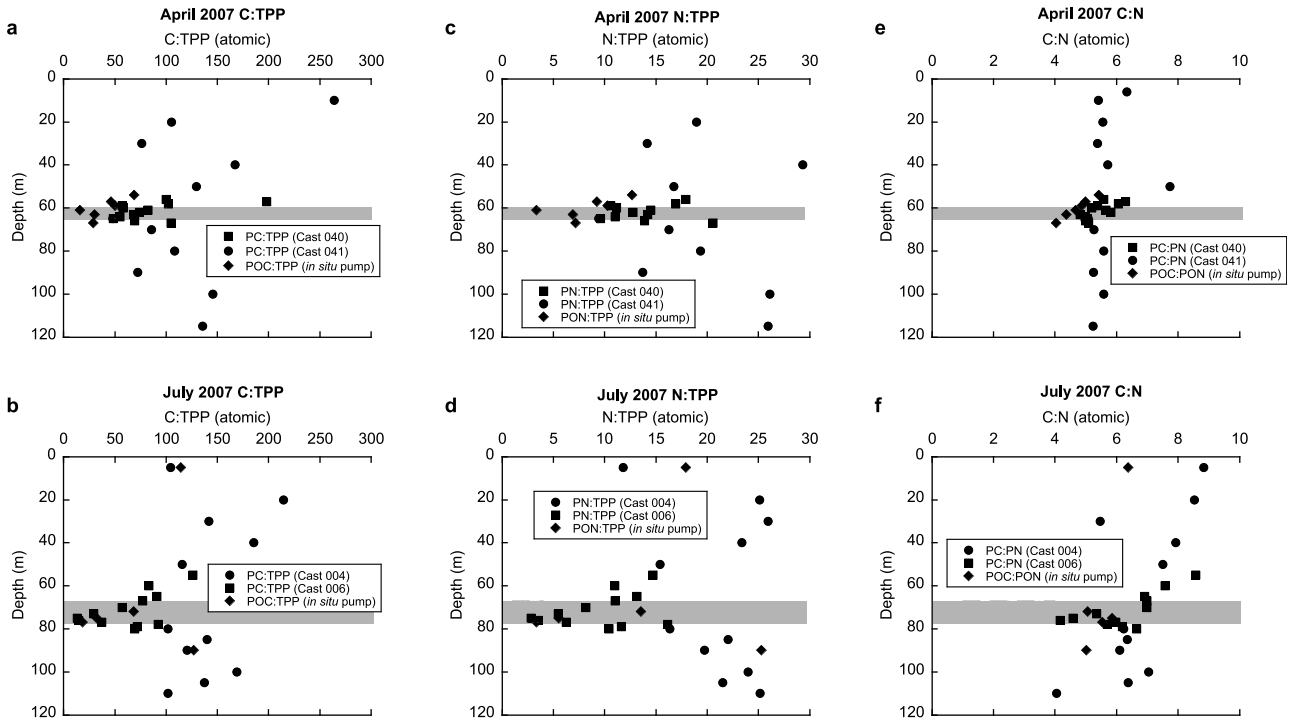

Figure 5. Particulate elemental ratios. Atomic ratios of particulate C, N, and P revealed that P is preferentially accumulated within the redox transition zone (shaded regions) in both sampling seasons. The experimental errors associated with the measurement of particulate C, N, and P were ±15%, ±6%, and ±5%, respectively.

degradation of endogenous inorganic poly-P is an important mechanism for redox-sensitive cycling of poly-P, rather than bacterial degradation of phytoplankton-associated poly-P, which is likely to be detected in a larger size fraction. However, our observations do not rule out phytoplankton-derived inorganic poly-P as an exogenous source of poly-P for remineralization by bacteria. For example, inorganic poly-P exists in a range of sizes, including micron-sized granules within 50–100 μm phytoplankton cells down to dissolved molecules (<0.45 μm) [*Diaz et al.*, 2008]. Although the bioavailability of exogenous inorganic poly-P remains largely unexplored, bacteria may potentially remineralize phytoplankton-derived particulate inorganic poly-P in the 1–10 μm particle fraction. Alternatively, dissolved poly-P may adsorb to the surface of bacterial cells where it may undergo further transformation, which is consistent with our finding of 23% excess accumulation of adsorbed organic P in the 1–10 μm particle fraction.

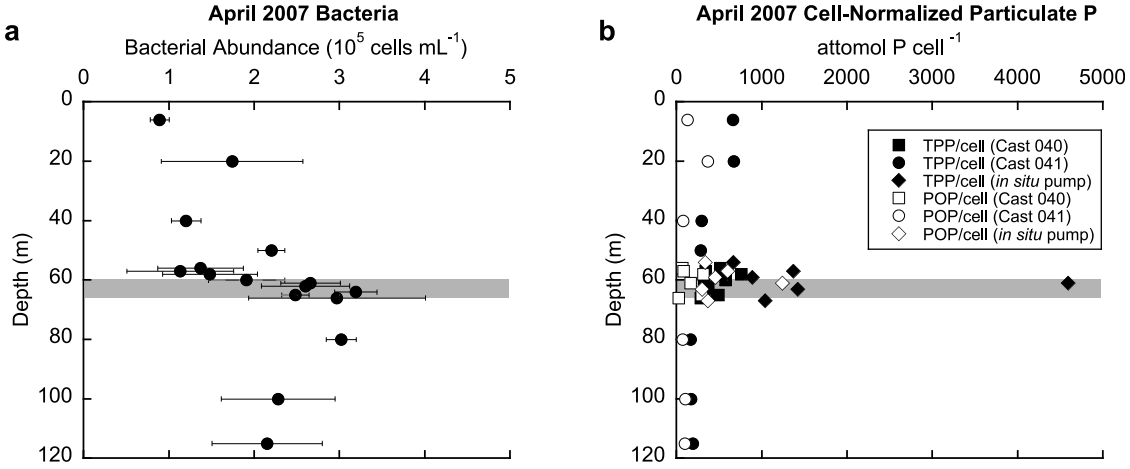

Figure 6. Bacterial abundance and cell-normalized phosphorus content. (a) Concentrations of bacteria in April 2007 peaked within the hypoxic transition zone (shaded region), as did (b) the concentration of cell-normalized total particulate P (TPP) and particulate organic P (POP). The error associated with the measurement of particulate P was typically less than ±5%.

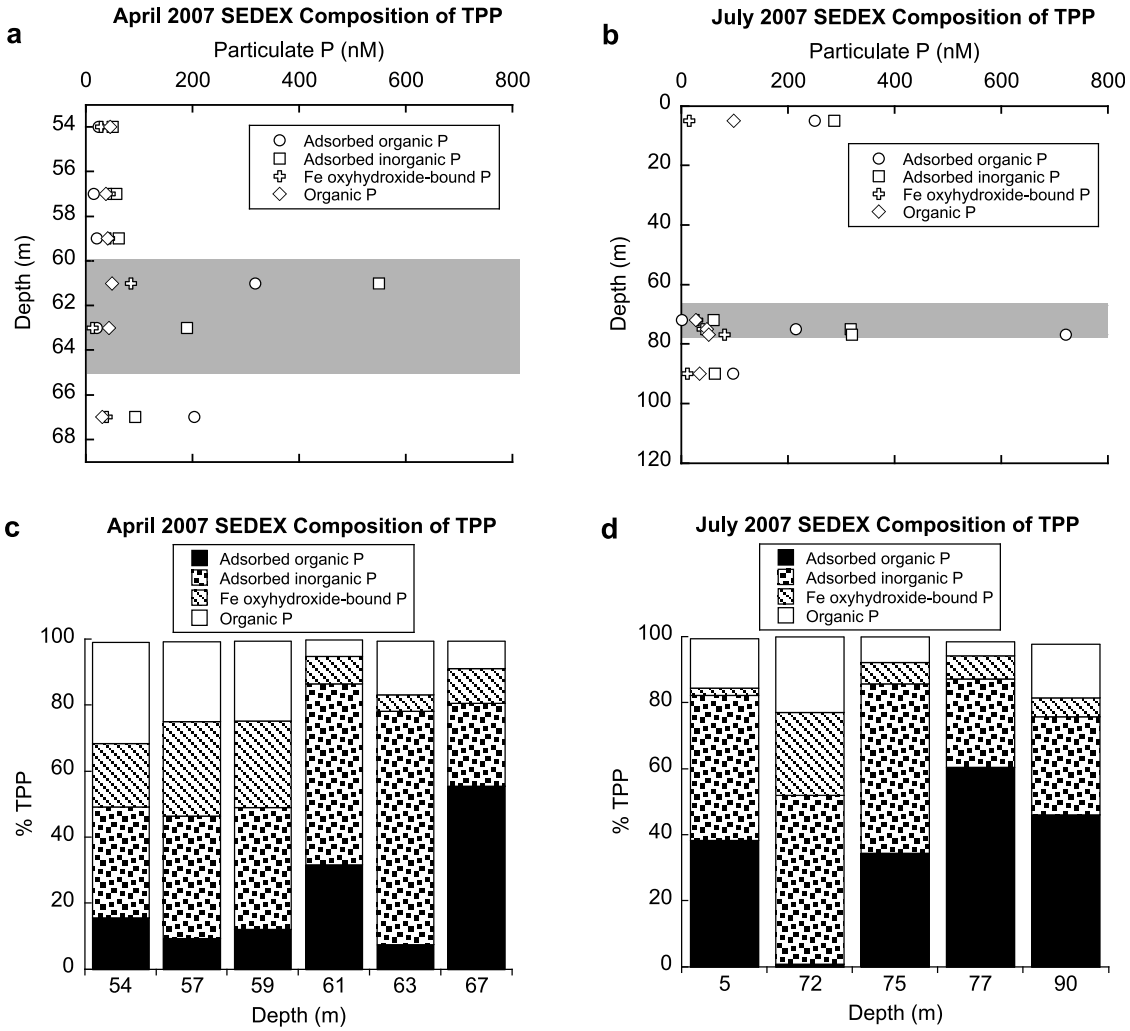

Figure 7. SEDEX composition of particulate phosphorus. Loosely adsorbed organic P accounted for approximately 23% of the non-Redfieldian accumulation of P within the particulate P maximum in both sampling seasons. The TPP maxima in April and July are represented by the sample at 61 m and 77 m in each season, respectively. Error associated with the measurement of organic P in SEDEX extracts was ±31%, whereas the error associated with the measurement of inorganic P in SEDEX extracts was ±24%.

3.4. Quantification of Mechanisms for Redox-Sensitive P Cycling in Suspended Particles (1–10 μm)

[29] Our direct field observations reveal a pattern of inorganic poly-P content in 1–10 μm particles that is consistent with the redox-sensitive transformation of poly-P. While the dissolution of poly-P is presumably a redox-independent process that cannot be ruled out, the spatial correlation between increasing hypoxia/anoxia and the disappearance of particulate poly-P tends to suggest redox-sensitive microbial remineralization of poly-P as a dominant process. Assuming this is the case, a quantitative understanding of the contribution of poly-P remineralization to redox-sensitive production of dissolved P can be obtained.

3.4.1. Vertical Dispersive Flux of SRP

[30] Several mechanisms may contribute to the maintenance of the sharp peak in SRP concentration at the hypoxic transition zone. These may include Fe-linked P cycling and microbial poly-P cycling. Assuming one-dimensional steady state, these SRP production mechanisms must collectively balance the vertical dispersive flux of SRP (D_v). Vertical advective transport of SRP across the well-stratified hypoxic transition zone in Effingham Inlet is considered negligible; therefore, vertical turbulent diffusion is assumed to be the main component of D_v. Vertical turbulent diffusion of SRP is thus calculated as the product of the vertical turbulent diffusivity constant (K_v) and the vertical gradient of SRP concentration across the hypoxic transition:

$$D_v = K_v \frac{d[SRP]}{dx} \quad (1)$$

where x is depth in meters. The vertical turbulent diffusive fluxes of SRP were calculated for every SRP profile by determining the SRP concentration gradient above the peak SRP concentration (Table 1). The vertical turbulent diffusivity constant was modeled using the density budget method

Table 1. Vertical Dispersive SRP Fluxes[a]

Month	Cast	Depth (m)	SRP (μmol m^{-3})	$\frac{d[SRP]}{dx}$ (μmol m^{-4})	Average K_v (m^2 d^{-1})	D_v (μmol m^{-2} d^{-1})
April	40	58	2570	1100	0.60	663
		60	4770			
July	3	72	3110	478	5.50	2625
		76	5020			
July	76	71	3390	213	5.06	1076
		75	4240			

[a]The vertical dispersive flux of SRP was calculated for each cast according to equation (1). Typical errors associated with the measurement of SRP were <±3%.

developed for stratified aquatic systems [*Axell*, 1998; *Gargett*, 1984; *Manning et al.*, 2010; *Turnewitsch and Pohl*, 2010]. Briefly, polynomial functions were fit to the average density profile collected in each sampling season using Matlab 7.10. The approach utilized our time series measurements of seawater density (i.e., July and April data sets) to calculate K_v as a function of depth by the following relationship:

$$K_v = \frac{\frac{d}{dt}\int_{x=b}^{x=a} \rho_{SW}\,dx}{\frac{d\rho_{SW}}{dx}|_{x=a}} \quad (2)$$

where ρ_{SW} is seawater density, a is the depth of interest, b is the total depth, and t is time.

[31] Across the SRP gradient, calculated values for K_v ranged from 1.5×10^{-5} m^2 s^{-1} to 17.5×10^{-5} m^2 s^{-1} and from 5.8×10^{-6} m^2 s^{-1} to 8.1×10^{-6} m^2 s^{-1} in the July and April sampling seasons, respectively. These values are in good agreement with the value of $5.2 \pm 0.7 \times 10^{-5}$ m^2 s^{-1} reported previously for Saanich Inlet [*Manning et al.*, 2010], a neighboring system of fjords on Vancouver Island, and values of 1.14×10^{-6} m^2 s^{-1} to 8.65×10^{-6} m^2 s^{-1} reported previously for well-stratified waters of the Baltic Sea's Eastern Gotland Basin [*Turnewitsch and Pohl*, 2010]. Average K_v values across the depth interval of interest were used in the calculation of D_v (Table 1). The vertical dispersion of SRP from its peak concentration in the hypoxic transition zone ranged from 663 to 2625 μmol m^{-2} d^{-1} throughout the April and July sampling seasons (Table 1).

3.4.2. Iron-Linked SRP Remobilization

[32] The reductive dissolution of Fe oxyhydroxide particles in hypoxic/anoxic waters is associated with the remobilization of SRP. To quantify this redox-sensitive P remobilization flux, the flux of reducible Fe production (F_{Fe}) was first calculated. F_{Fe} is defined as the product of the change in total particulate Fe concentration across the redox boundary ($\Delta Fe_{P,Tot}$) and the vertical settling flux of Fe oxyhydroxide particles estimated by Stoke's Law:

$$F_{Fe} = \Delta Fe_{P,Tot}\left(\frac{\rho_{Fe} - \rho_{SW}}{18\mu} g d_{Fe}^2\right) \quad (3)$$

where ρ_{Fe} is the average density of Fe oxyhydroxide particles, g is acceleration due to gravity, d_{Fe} is the average diameter of Fe oxyhydroxide particles, and μ is the dynamic viscosity of seawater. Because particles were size fractionated between 1 and 10 μm, F_{Fe} was computed at both end-member values of d_{Fe}. A minimum average Fe oxyhydroxide particle density of 2.82 ± 0.26 g cm^{-3} was assumed to be representative of particles of this size range [*Schwertmann and Fischer*, 1973; *Taillefert and Gaillard*, 2002], whereas 5.50 g cm^{-3} (hematite) was defined as the maximum average density. The dynamic viscosity of seawater was calculated by the equation described by *Sharqawy et al.* [2010] using in situ temperature, density, and salinity measurements.

Table 2. Iron-Linked P Remobilization[a]

Month	Depth (m)	$Fe_{p,Tot}$ (μmol m^{-3})	P:Fe (Atomic)	$F_{SRP,Fe}$ (μmol m^{-2} d^{-1}; % SRP Flux): Maximum Size Scenario (d_{Fe} = 10 μm)		$F_{SRP,Fe}$ (μmol m^{-2} d^{-1}; % SRP Flux): Minimum Size Scenario (d_{Fe} = 1 μm)	
				Max Density Scenario (ρ_{Fe} = 5.50 g cm^{-3})	Min Density Scenario (ρ_{Fe} = 2.28 g cm^{-3})	Max Density Scenario (ρ_{Fe} = 5.50 g cm^{-3})	Min Density Scenario (ρ_{Fe} = 2.28 g cm^{-3})
April 2007	54	171.0	0.17	423 (64%)	170 (26%)	4.2 (0.6%)	1.7 (0.3%)
	57	181.5	0.24	651 (98%)	261 (39%)	6.5 (1.0%)	2.6 (0.4%)
	59	178.6	0.25	645 (97%)	259 (39%)	6.5 (1.0%)	2.6 (0.4%)
	61	76.6	0.57	638 (96%)	256 (37%)	6.4 (1.0%)	2.6 (0.4%)
July 2007	72	176.5	0.17	438 (24%)	176 (10%)	4.4 (0.2%)	1.8 (0.1%)
	75	172.1	0.23	590 (32%)	236 (13%)	5.9 (0.3%)	2.4 (0.1%)
	77	160.6	0.32	761 (41%)	305 (17%)	7.6 (0.4%)	3.1 (0.2%)
Average				592 (65%)	238 (26%)	5.9 (0.6%)	2.4 (0.3%)
±SD				±122 (33%)	±49 (13%)	±1.2 (0.3%)	±0.5 (0.1%)

[a]The flux of dissolved P associated with the reductive dissolution of Fe oxyhydroxide particles was calculated for each depth sampled according to equations (3) and (4) and under different particle size and density scenarios. Each flux is expressed in absolute terms (μmol m^{-2} d^{-1}) and relative to the average vertical dispersive flux of SRP in the respective sampling season (% SRP flux). Typical errors associated with the measurement of total particulate Fe were ±5–10%.

Table 3. Redox-Sensitive Microbial Cycling of Inorganic Poly-P[a]

Month	Depth (m)	Inorganic Poly-P (μmol P m^{-3})	$F_{SRP,PAB}$ (μmol m^{-2} d^{-1}; % SRP Flux): Maximum Size Scenario (d_{PAB} = 10 μm)		$F_{SRP,PAB}$ (μmol m^{-2} d^{-1}; % SRP Flux): Minimum Size Scenario (d_{PAB} = 1 μm)	
			Maximum Density Scenario (ρ_{PAB} = 12.0 × ρ_{SW})	Minimum Density Scenario (ρ_{PAB} = 5.5 × ρ_{SW})	Maximum Density Scenario (ρ_{PAB} = 12.0 × ρ_{SW})	Minimum Density Scenario (ρ_{PAB} = 5.5 × ρ_{SW})
April 2007	59	1	37 (6%)	15 (2%)	0.4 (0.1%)	0.2 (0.0%)
July 2007	75	2	74 (4%)	30 (2%)	0.7 (0.0%)	0.3 (0.0%)
	77	9	331 (18%)	136 (7%)	3.3 (0.2%)	1.4 (0.1%)
Average			147 (9%)	60 (4%)	1.5 (0.1%)	0.6 (0.0%)
±SD			±160 (8%)	±66 (3%)	±1.6 (0.1%)	±0.7 (0.0%)

[a]The flux of dissolved P associated with the redox-sensitive cycling of inorganic poly-P by bacteria was calculated for each depth sampled according to equation (5) and under different cell size and density scenarios. Each flux is expressed in absolute terms (μmol m^{-2} d^{-1}) and relative to the average vertical dispersive flux of SRP in the respective sampling season (% SRP flux). Typical errors associated with the measurement of inorganic poly-P are ±15%.

Total particulate Fe concentrations below the redox transition were below the detection limit of our analytical system and were therefore assumed to be equal to zero for the purpose of these calculations.

[33] The remobilization of SRP associated with the reductive dissolution of Fe oxyhydroxide particles ($F_{SRP,\ Fe}$) was determined by multiplying the flux of reducible iron production, defined above, by the atomic ratio of P to Fe:

$$F_{SRP,Fe} = \frac{P}{Fe} \times F_{Fe} \tag{4}$$

The atomic ratio of P to Fe was determined experimentally (Table 2). Under the maximum particle size scenario, the values for $F_{SRP,Fe}$ ranged from 238 ± 49 μmol m^{-2} d^{-1} (minimum density) to 592 ± 122 μmol m^{-2} d^{-1} (maximum density) across both seasons (Table 2). These fluxes account for 26 ± 13% and 65 ± 33% of the average SRP diffusive flux determined above (Tables 1 and 2). Under the minimum particle size scenario, however, $F_{SRP,Fe}$ values were two orders of magnitude lower, accounting for less than 1% of the vertical dispersive transport of SRP across the hypoxic transition zone on average (Table 2).

3.4.3. Microbial Cycling of Inorganic Poly-P

[34] Redox-sensitive remobilization of inorganic poly-P is generally thought to be a microbially regulated process. For example, the microbial breakdown of endogenous inorganic poly-P under hypoxic/anoxic stress in industrial aquatic systems such as wastewater treatment reactors is associated with the release of SRP to the surrounding environment, with nucleotides serving as likely intermediates [*Brown and Kornberg*, 2004; *Kornberg*, 1995; *Rao et al.*, 2009; *Groenestijn et al.*, 1987]. Inorganic poly-P not only functions as an energy reserve but can also serve as ballast in bacterial cells [*Romans et al.*, 1994]. For example, negatively buoyant polyphosphate-laden cells of the cyanobacterial species *Trichodesmium tenue* have been found to be 5.5–12.0 times as dense as positively buoyant, polyphosphate-free cells of the same species [*Romans et al.*, 1994].

[35] Although we did not directly observe poly-P accumulating bacteria (PAB) in Effingham Inlet, the finding of inorganic poly-P in the 1–10 μm particulate fraction is consistent with their presence. To quantify redox-sensitive SRP remobilization by the hypothesized community of PAB in Effingham Inlet ($F_{SRP,PAB}$), the change in inorganic poly-P content across the redox transition zone ($\Delta polyP$) is multiplied by the vertical settling velocity of negatively buoyant PAB:

$$F_{SRP,PAB} = \Delta polyP\left(\frac{\rho_{PAB} - \rho_{SW}}{18\mu} g d_{PAB}^2\right) \tag{5}$$

where ρ_{PAB} is the average density of PAB (g cm^{-3}) and d_{PAB} is the average diameter of PAB. Because of the 1–10 μm size fractionation of our samples, these end-member particle diameters were used to define d_{PAB} for minimum and maximum particle size scenarios. Microscopic images from the analysis of PAB in natural populations, laboratory cultures, as well as sewage treatment reactors show that PAB may form aggregates up to approximately 5–15 μm in diameter [*Eixler et al.*, 2005; *Liu et al.*, 2001; *Selig et al.*, 2004], likely in association with organic debris. For a minimum density scenario, the value of ρ_{PAB} was set to 5.5 times the ambient seawater density, i.e., 5.5 times the neutrally buoyant case. Similarly, a maximum density scenario was performed by setting ρ_{PAB} equal to 12.0 times the neutrally buoyant case. Direct measurements of the buoyancy of PAB are very limited; however, these density values are consistent with measurements made previously by *Romans et al.* [1994] on the cyanobacterium *T. tenue.* As inorganic poly-P concentrations below the hypoxic transition zone were lower than our analytical detection limit (<0.8 nM in situ), a concentration of zero was assumed for inorganic poly-P below the hypoxic zone.

[36] Under the maximum cell size scenario, SRP remobilization by the redox-sensitive microbial breakdown of inorganic poly-P was estimated to be 37–331 μmol m^{-2} d^{-1} (maximum cell density scenario) and 15–136 μmol m^{-2} d^{-1} (minimum cell density scenario) across both sampling seasons (Table 3). Thus, inorganic poly-P degradation accounted for as much as 4 ± 3% to 9 ± 8% of the vertical dispersive SRP flux (Table 3). Relative to their magnitudes, these fluxes display a much larger variation with respect to depth than that seen in the Fe-linked P remobilization fluxes (Table 2), suggesting that redox-sensitive microbial metabolism of inorganic poly-P occurs at an overlapping yet much narrower range of dissolved oxygen concentrations than reductive dissolution of Fe oxyhydroxides. Therefore, the depth-averaged estimates of inorganic poly-P degradation provided above may not accurately represent the contribution of this mechanism to the

remobilization of P across the redox transition in Effingham Inlet. For example, in the TPP max measured during July 2007, particulate inorganic poly-P degradation in the 1–10 μm size fraction could account for as much as 18% (maximum cell size and density scenario) of the total vertical dispersive flux of SRP (Table 3).

4. Perspectives and Implications

[37] Maxima in SRP and TPP content were observed within the water column redox transition zone of Effingham Inlet during April and July 2007. TPP maxima were characterized by a preferential accumulation of loosely adsorbed organic P in both sampling seasons. This P fraction perhaps contained a substantial amount of inorganic poly-P, which is typically detected in operationally defined "organic P" pools. Based on our modeling approach, the redox-sensitive cycling of P linked to Fe oxyhydroxide dissolution could not account for the production of SRP at the hypoxic interface. Inorganic poly-P may therefore be involved in the redox-sensitive production of SRP. Based on conservative direct measurements of inorganic poly-P content, the redox-sensitive remineralization of poly-P can account for up to 4 $\pm$ 3% to 9 $\pm$ 8% of the vertical turbulent diffusive flux of SRP. This figure is likely a minimum estimate based on several issues related to our direct measurement of inorganic poly-P content. For example, our calculated poly-P remineralization fluxes may be substantially underestimated if a large fraction of the endogenous microbial inorganic poly-P pool is below 15 P units in length, as our quantification method is insensitive to these shorter-chain poly-P molecules [*Diaz and Ingall*, 2010]. Previous results also indicate that synthetic dissolved inorganic poly-P up to 130 P units in length is unstable over storage periods exceeding 10–15 days [*Diaz and Ingall*, 2010]. Thus, our particulate inorganic poly-P samples may have been compromised over longer periods of storage time ($\sim$years). Indeed, excess ($\sim$23%) accumulation of the adsorbed organic P SEDEX fraction within the TPP maximum indicates that the pool of redox-sensitive biogenic P may be larger than that indicated by direct measurements of inorganic poly-P. Furthermore, the steady state concentration of inorganic poly-P in microbial cells under oxygen stress may be vanishingly small if turnover rates are high, which would mask a potentially large role for poly-P in the redox-sensitive remobilization of SRP.

[38] Based on our calculations of Fe-linked P cycling and inorganic poly-P cycling, a maximum of only 74.3 $\pm$ 33.6% of the vertical dispersive SRP flux could be explained across both sampling seasons. The inability to account for the entire vertical dispersive flux of SRP by the combined fluxes of Fe-linked P cycling and poly-P cycling is furthermore consistent with an underestimation of poly-P flux. Less likely is the conclusion that our estimates of Fe-linked P cycling are substantially underestimated. For example, although the calculation of Fe-linked P remobilization fluxes in Effingham Inlet would benefit from experimental characterization of Fe oxyhydroxide particle size distributions, our estimates of Fe-linked P cycling are similar to those observed in other marine systems. Previous estimates in hypoxic regions of the Baltic Sea, for instance, showed that the contribution of oxyhydroxide-linked P cycling to water column dispersive fluxes of SRP ranged from 37 $\pm$ 45% to 62 $\pm$ 29% [*Turnewitsch and Pohl*, 2010].

[39] Based on our conservative estimates, microbial cycling of inorganic poly-P may contribute to the redox-sensitive remobilization of SRP in Effingham Inlet. The contribution of redox-sensitive poly-P cycling may be more substantial in other hypoxic/anoxic boundaries, especially iron-poor oxygen minimum zones of the open ocean and bacterial mat communities of known inorganic poly-P producers, such as *Thiomargarita namibiensis* [*Schulz and Schulz*, 2005] and closely related genera. The potential role of inorganic poly-P in the redox-sensitive cycling of P implies a direct biological mechanism for the enhanced release of P observed in hypoxic/anoxic environments, a phenomenon that has been predominantly explained by abiotic or indirect biological mechanisms for over half a century. The potential role of poly-P in the redox-sensitive remobilization of P also implies that natural PAB communities may contribute to a direct biological negative feedback mechanism for atmospheric oxygen stabilization over geologic timescales [*Van Cappellen and Ingall*, 1996]. In addition, through mechanisms of redox-sensitive poly-P cycling, organisms may form a positive feedback to eutrophication and the expansion of the world's oxygen minimum zones over shorter timescales.

[40] **Acknowledgments.** This material is based upon work supported by the National Science Foundation under grants 0526178 and 1060884. Thank you to Captain Ray McQuin and the crew of the R/V *Barnes*, Rick Keil and John Nuwer for assistance with field sampling, Susan Herron and Gabrielle Lyons for help during field sampling and sample analysis, and Renée Styles and Wendy Plessinger for assistance with sample analysis. Thank you also to George Patterson and John Platenius of the Clayoquot Field Station in Tofino, British Columbia, for providing lab space and a welcoming base for our field studies and to Meg Grantham for assistance in the use of the flame atomic adsorption spectrometer.

References

Algeo, T. J., and E. Ingall (2007), Sedimentary C_{org}: P ratios, paleocean ventilation, and Phanerozoic atmospheric pO_2, *Palaeogeogr. Palaeoclimatol. Palaeoecol.*, *256*(3–4), 130–155, doi:10.1016/j.palaeo.2007.02.029.

Anderson, L. A., and J. L. Sarmiento (1994), Redfield ratios of remineralization determined by nutrient data analysis, *Global Biogeochem. Cycles*, *8*(1), 65–80, doi:10.1029/93GB03318.

Aschar-Sobbi, R., A. Y. Abramov, C. Diao, M. E. Kargacin, G. J. Kargacin, R. J. French, and E. Pavlov (2008), High sensitivity, quantitative measurements of polyphosphate using a new DAPI-based approach, *J. Fluoresc.*, *18*(5), 859–866, doi:10.1007/s10895-008-0315-4.

Aspila, K. I., H. Agemian, and A. S. Y. Chau (1976), A semi-automated method for determination of inorganic, organic, and total phosphate in sediments, *Analyst*, *101*(1200), 187–197, doi:10.1039/an9760100187.

Axell, L. B. (1998), On the variability of Baltic Sea deepwater mixing, *J. Geophys. Res.*, *103*(C10), 21,667–21,682, doi:10.1029/98JC01714.

Benitez-Nelson, C. R. (2000), The biogeochemical cycling of phosphorus in marine systems, *Earth Sci. Rev.*, *51*(1–4), 109–135, doi:10.1016/S0012-8252(00)00018-0.

Broecker, W. S. (1982), Ocean chemistry during glacial time, *Geochim. Cosmochim. Acta*, *46*(10), 1689–1705, doi:10.1016/0016-7037(82)90110-7.

Brown, M. R. W., and A. Kornberg (2004), Inorganic polyphosphate in the origin and survival of species, *Proc. Natl. Acad. Sci. U. S. A.*, *101*(46), 16,085–16,087, doi:10.1073/pnas.0406909101.

Codispoti, L. A., J. A. Brandes, J. P. Christensen, A. H. Devol, S. W. A. Naqvi, H. W. Paerl, and T. Yoshinari (2001), The oceanic fixed nitrogen and nitrous oxide budgets: Moving targets as we enter the anthropocene?, *Sci. Mar.*, *65*, 85–105, doi:10.3989/scimar.2001.65s285.

Comeau, Y., K. J. Hall, R. E. W. Hancock, and W. K. Oldham (1986), Biochemical model for enhanced biological phosphorus removal, *Water Res.*, *20*(12), 1511–1521, doi:10.1016/0043-1354(86)90115-6.

Davelaar, D. (1993), Ecological significance of bacterial polyphosphate metabolism in sediments, *Hydrobiologia*, *253*(1–3), 179–192, doi:10.1007/BF00050737.

Diaz, J. M., and E. D. Ingall (2010), Fluorometric quantification of natural inorganic polyphosphate, *Environ. Sci. Technol.*, *44*(12), 4665–4671, doi:10.1021/es100191h.

Diaz, J., E. Ingall, C. Benitez-Nelson, D. Paterson, M. D. de Jonge, I. McNulty, and J. A. Brandes (2008), Marine polyphosphate: A key player in geologic phosphorus sequestration, *Science*, *320*(5876), 652–655, doi:10.1126/science.1151751.

Eixler, S., U. Selig, and U. Karsten (2005), Extraction and detection methods for polyphosphate storage in autotrophic planktonic organisms, *Hydrobiologia*, *533*, 135–143, doi:10.1007/s10750-004-2406-9.

Froelich, P. N., G. P. Klinkhammer, M. L. Bender, N. A. Luedtke, G. R. Heath, D. Cullen, P. Dauphin, D. Hammond, B. Hartman, and V. Maynard (1979), Early oxidation of organic matter in pelagic sediments of the eastern equatorial Atlantic: Suboxic diagenesis, *Geochim. Cosmochim. Acta*, *43*(7), 1075–1090, doi:10.1016/0016-7037(79)90095-4.

Gächter, R., J. S. Meyer, and A. Mares (1988), Contribution of bacteria to release and fixation of phosphorus in lake sediments, *Limnol. Oceanogr.*, *33*, 1542–1558, doi:10.4319/lo.1988.33.6_part_2.1542.

Gargett, A. E. (1984), Vertical eddy diffusivity in the ocean interior, *J. Mar. Res.*, *42*, 359–393, doi:10.1357/002224084788502756.

Golterman, H. L. (2001), Phosphate release from anoxic sediments or 'What did Mortimer really write?', *Hydrobiologia*, *450*, 99–106, doi:10.1023/A:1017559903404.

Groenestijn, J. W., M. H. Deinema, and A. J. B. Zehnder (1987), ATP production from polyphosphate in *Acinetobacter* strain 210A, *Arch. Microbiol.*, *148*(1), 14–19, doi:10.1007/BF00429640.

Hansen, H. P., and F. Koroleff (1999), Determination of dissolved inorganic phosphate, in *Methods of Seawater Analysis*, edited by K. Grasshoff et al., pp. 170–174, John Wiley, New York.

Hedges, J. I., and J. H. Stern (1984), Carbon and nitrogen determinations of carbonate-containing solids, *Limnol. Oceanogr.*, *29*(3), 657–663, doi:10.4319/lo.1984.29.3.0657.

Hupfer, M., R. Gächter and H. Rüeggger (1995), Polyphosphate in lake sediments: ^{31}P NMR spectroscopy as a tool for its identification, *Limnol. Oceanogr.*, *40*(3), 610–617, doi:10.4319/lo.1995.40.3.0610.

Hupfer, M., B. Rübe, and P. Schmieder (2004), Origin and diagenesis of polyphosphate in lake sediments: A ^{31}P-NMR study, *Limnol. Oceanogr.*, *49*(1), 1–10, doi:10.4319/lo.2004.49.1.0001.

Hupfer, M., S. Glöss, P. Schmieder, and H.-P. Grossart (2008), Methods for detection and quantification of polyphosphate and polyphosphate accumulating microorganisms in aquatic sediments, *Int. Rev. Hydrobiol.*, *93*(1), 1–30, doi:10.1002/iroh.200610935.

Ingall, E., and R. Jahnke (1994), Evidence for enhanced phosphorus regeneration from marine sediments overlain by oxygen depleted waters, *Geochim. Cosmochim. Acta*, *58*(11), 2571–2575, doi:10.1016/0016-7037(94)90033-7.

Ingall, E., and R. Jahnke (1997), Influence of water-column anoxia on the elemental fractionation of carbon and phosphorus during sediment diagenesis, *Mar. Geol.*, *139*(1–4), 219–229, doi:10.1016/S0025-3227(96)00112-0.

Ingall, E. D., R. M. Bustin, and P. Van Cappellen (1993), Influence of water column anoxia on the burial and preservation of carbon and phosphorus in marine shales, *Geochim. Cosmochim. Acta*, *57*(2), 303–316, doi:10.1016/0016-7037(93)90433-W.

Ingall, E., L. Kolowith, T. Lyons, and M. Hurtgen (2005), Sediment carbon, nitrogen and phosphorus cycling in an anoxic fjord, Effingham Inlet, British Columbia, *Am. J. Sci.*, *305*(3), 240–258, doi:10.2475/ajs.305.3.240.

Jilbert, T., C. P. Slomp, B. G. Gustafsson, and W. Boer (2011), Beyond the Fe–P-redox connection: Preferential regeneration of phosphorus from organic matter as a key control on Baltic Sea nutrient cycles, *Biogeosci. Discuss.*, *8*, 655–706, doi:10.5194/bgd-8-655-2011.

Kornberg, A. (1995), Inorganic polyphosphate: Toward making a forgotten polymer unforgettable, *J. Bacteriol.*, *177*(3), 491–496.

Kornberg, A., N. N. Rao, and D. Ault-Riché (1999), Inorganic polyphosphate: A molecule of many functions, *Annu. Rev. Biochem.*, *68*, 89–125, doi:10.1146/annurev.biochem.68.1.89.

Liu, W.-T., A. T. Nielsen, J.-H. Wu, C.-S. Tsai, Y. Matsuo, and S. Molin (2001), *In situ* identification of polyphosphate- and polyhydroxyalkanoate-accumulating traits for microbial populations in a biological phosphorus removal process, *Environ. Microbiol.*, *3*(2), 110–122, doi:10.1046/j.1462-2920.2001.00164.x.

Liu, Z. F., G. Stewart, J. K. Cochran, C. Lee, R. A. Armstrong, D. J. Hirschberg, B. Gasser, and J.-C. Miquel (2005), Why do POC concentrations measured using Niskin bottle collections sometimes differ from those using in-situ pumps?, *Deep Sea Res., Part I*, *52*(7), 1324–1344, doi:10.1016/j.dsr.2005.02.005.

Liu, Z. F., J. K. Cochran, C. Lee, B. Gasser, J. C. Miquel, and S. G. Wakeham (2009), Further investigations on why POC concentrations differ in samples collected by Niskin bottle and in situ pump, *Deep Sea Res., Part II*, *56*(18), 1558–1567, doi:10.1016/j.dsr2.2008.12.019.

Manning, C. C., R. C. Hamme, and A. Bourbonnais (2010), Impact of deep-water renewal events on fixed nitrogen loss from seasonally-anoxic Saanich Inlet, *Mar. Chem.*, *122*(1–4), 1–10, doi:10.1016/j.marchem.2010.08.002.

McManus, J., W. M. Berelson, K. H. Coale, K. S. Johnson, and T. E. Kilgore (1997), Phosphorus regeneration in continental margin sediments, *Geochim. Cosmochim. Acta*, *61*(14), 2891–2907, doi:10.1016/S0016-7037(97)00138-5.

Moran, S. B., M. A. Charette, S. M. Pike, and C. A. Wicklund (1999), Differences in seawater particulate organic carbon concentration in samples collected using small- and large-volume methods: The importance of DOC adsorption to the filter blank, *Mar. Chem.*, *67*(1–2), 33–42, doi:10.1016/S0304-4203(99)00047-X.

Mortimer, C. H. (1941), The exchange of dissolved substances between mud and water in lakes, *J. Ecol.*, *29*, 280–329, doi:10.2307/2256395.

Mortimer, C. H. (1942), The exchange of dissolved substances between mud and water in lakes, *J. Ecol.*, *30*, 147–201, doi:10.2307/2256691.

Naqvi, S. W. A., D. A. Jayakumar, P. V. Narvekar, H. Naik, V. Sarma, W. D'Souza, S. Joseph, and M. D. George (2000), Increased marine production of N_2O due to intensifying anoxia on the Indian continental shelf, *Nature*, *408*, 346–349, doi:10.1038/35042551.

Nielsen, P. H., A. T. Mielczarek, C. Kragelund, J. L. Nielsen, A. M. Saunders, Y. H. Kong, A. A. Hansen, and J. Vollertsen (2010), A conceptual ecosystem model of microbial communities in enhanced biological phosphorus removal plants, *Water Res.*, *44*(17), 5070–5088, doi:10.1016/j.watres.2010.07.036.

Paytan, A., and K. McLaughlin (2007), The oceanic phosphorus cycle, *Chem. Rev.*, *107*(2), 563–576, doi:10.1021/cr0503613.

Planavsky, N. J., O. J. Rouxel, A. Bekker, S. V. Lalonde, K. O. Konhauser, C. T. Reinhard, and T. W. Lyons (2010), The evolution of the marine phosphate reservoir, *Nature*, *467*, 1088–1090, doi:10.1038/nature09485.

Rabalais, N. N., R. E. Turner, and W. J. Wiseman (2001), Hypoxia in the Gulf of Mexico, *J. Environ. Qual.*, *30*(2), 320–329, doi:10.2134/jeq2001.302320x.

Rabalais, N. N., R. E. Turner, Q. Dortch, D. Justic, V. J. Bierman, and W. J. Wiseman (2002), Nutrient-enhanced productivity in the northern Gulf of Mexico: Past, present and future, *Hydrobiologia*, *475-476*(1), 39–63, doi:10.1023/A:1020388503274.

Rao, N. N., M. R. Gomez-Garcia, and A. Kornberg (2009), Inorganic polyphosphate: Essential for growth and survival, *Annu. Rev. Biochem.*, *78*, 605–647, doi:10.1146/annurev.biochem.77.083007.093039.

Redfield, A. C. (1958), The biological control of chemical factors in the environment, *Am. Sci.*, *46*(3), 205–221.

Romans, K. M., E. J. Carpenter, and B. Bergman (1994), Buoyancy regulation in the colonial diazotrophic cyanobacterium *Trichodesmium tenue*: Ultrastructure and storage of carbohydrate, polyphosphate, and nitrogen, *J. Phycol.*, *30*(6), 935–942, doi:10.1111/j.0022-3646.1994.00935.x.

Ruttenberg, K. C. (1992), Development of a sequential extraction method for different forms of phosphorus in marine sediments, *Limnol. Oceanogr.*, *37*(7), 1460–1482, doi:10.4319/lo.1992.37.7.1460.

Sannigrahi, P., and E. Ingall (2005), Polyphosphates as a source of enhanced P fluxes in marine sediments overlain by anoxic waters: Evidence from ^{31}P NMR, *Geochem. Trans.*, *6*(3), 52–59, doi:10.1186/1467-4866-6-52.

Savchuk, O. P., F. Wulff, S. Hille, C. Humborg, and F. Pollehne (2008), The Baltic Sea a century ago—A reconstruction from model simulations, verified by observations, *J. Mar. Syst.*, *74*(1–2), 485–494, doi:10.1016/j.jmarsys.2008.03.008.

Schuler, A. J., and D. Jenkins (2003), Enhanced biological phosphorus removal from wastewater by biomass with different phosphorus contents, part II: Anaerobic adenosine triphosphate utilization and acetate uptake rates, *Water Environ. Res.*, *75*(6), 499–511, doi:10.2175/106143003X141295.

Schulz, H. N., and H. D. Schulz (2005), Large sulfur bacteria and the formation of phosphorite, *Science*, *307*(5708), 416–418, doi:10.1126/science.1103096.

Schwertmann, U., and W. R. Fischer (1973), Natural "amorphous" ferric hydroxide, *Geoderma*, *10*, 237–247, doi:10.1016/0016-7061(73)90066-9.

Selig, U., T. Hübener, R. Heerkloss, and H. Schubert (2004), Vertical gradient of nutrients in two dimictic lakes—Influence of phototrophic sulfur bacteria on nutrient balance, *Aquat. Sci.*, *66*(3), 247–256, doi:10.1007/s00027-004-0684-y.

Seviour, R. J., T. Mino, and M. Onuki (2003), The microbiology of biological phosphorus removal in activated sludge systems, *FEMS Microbiol. Rev.*, *27*(1), 99–127, doi:10.1016/S0168-6445(03)00021-4.

Sharqawy, M. H., J. H. Lienhard V, and S. M. Zubair (2010), Thermophysical properties of seawater: A review of existing correlations and data, *Desalin. Water Treat.*, *16*, 354–380, doi:10.5004/dwt.2010.1079.

Slomp, C. P., J. Thomson, and G. J. de Lange (2002), Enhanced regeneration of phosphorus during formation of the most recent eastern Mediterranean sapropel (S1), *Geochim. Cosmochim. Acta*, *66*(7), 1171–1184, doi:10.1016/S0016-7037(01)00848-1.

Stramma, L., G. C. Johnson, J. Sprintall, and V. Mohrholz (2008), Expanding oxygen-minimum zones in the tropical oceans, *Science*, *320*(5876), 655–658, doi:10.1126/science.1153847.

Sundby, B., C. Gobeil, N. Silverberg, and A. Mucci (1992), The phosphorus cycling in coastal marine sediments, *Limnol. Oceanogr.*, *37*(6), 1129–1145, doi:10.4319/lo.1992.37.6.1129.

Taillefert, M., and J.-F. Gaillard (2002), Reactive transport modeling of trace elements in the water column of a stratified lake: Iron cycling and metal scavenging, *J. Hydrol.*, *256*, 16–34, doi:10.1016/S0022-1694(01)00524-8.

Turnewitsch, R., and C. Pohl (2010), An estimate of the efficiency of the iron- and manganese-driven dissolved inorganic phosphorus trap at an oxic/euxinic water column redoxcline, *Global Biogeochem. Cycles*, *24*, GB4025, doi:10.1029/2010GB003820.

Vahtera, E., et al. (2007), Internal ecosystem feedbacks enhance nitrogen-fixing cyanobacteria blooms and complicate management in the Baltic Sea, *Ambio*, *36*(2), 186–194, doi:10.1579/0044-7447(2007)36[186:IEFENC]2.0.CO;2.

Van Cappellen, P., and E. D. Ingall (1996), Redox stabilization of the atmosphere and oceans by phosphorus-limited marine productivity, *Science*, *271*(5248), 493–496, doi:10.1126/science.271.5248.493.

Young, C. L., and E. D. Ingall (2010), Marine dissolved organic phosphorus composition: Insights from samples recovered using combined electrodialysis/reverse osmosis, *Aquat. Geochem.*, *16*(4), 563–574, doi:10.1007/s10498-009-9087-y.